Pulmonary alveolar microlithiasis

Patrick Kosciuk[1], Cristopher Meyer[2], Kathryn A. Wikenheiser-Brokamp[3,4] and Francis X. McCormack[1]

Number 3 in the Series "Ultra-rare lung disease"
Edited by Sergio Harari and Marc Humbert

Affiliations: [1]Division of Pulmonary, Critical Care, and Sleep Medicine, University of Cincinnati, Cincinnati, OH, USA. [2]Division of Radiology, University of Wisconsin, Madison, WI, USA. [3]Division of Pathology & Laboratory Medicine, Cincinnati Children's Hospital Medical Center, Cincinnati, OH, USA. [4]Dept of Pathology & Laboratory Medicine, University of Cincinnati, Cincinnati, OH, USA.

Correspondence: Francis X. McCormack, Division of Pulmonary, Critical Care and Sleep Medicine, University of Cincinnati, MSB 6165, 231 Albert Sabin Way, Cincinnati, OH 45267-0564, USA. E-mail: frank.mccormack@uc.edu

@ERSpublications
A review of the epidemiology and molecular pathophysiology of pulmonary alveolar microlithiasis https://bit.ly/3lBgM7p

Cite this article as: Kosciuk P, Meyer C, Wikenheiser-Brokamp KA, *et al*. Pulmonary alveolar microlithiasis. *Eur Respir Rev* 2020; 29: 200024 [https://doi.org/10.1183/16000617.0024-2020].

ABSTRACT Pulmonary alveolar microlithiasis (PAM) is a fascinating rare lung disease that is associated with the accumulation of hydroxyapatite microliths within the lumen of the alveolar spaces. In most patients, PAM is discovered incidentally on radiographs performed for other purposes, and the typical disease course is characterised by slowly progressive respiratory insufficiency over decades. Recent genetic analyses that have revealed that the deficiency of the sodium-phosphate cotransporter NPT2B is the cause of PAM have enabled the development of powerful animal models that inform our approach to disease management and treatment. Here we review the epidemiology and molecular pathophysiology of PAM, as well as the diagnostic approach, clinical manifestations, radiographic and pathologic features, and clinical management of the disease. Although there are no proven treatments for PAM, progress in our understanding of disease pathogenesis is providing insights that suggest strategies for trials.

Introduction

Pulmonary alveolar microlithiasis (PAM) is a rare hereditary disease of abnormal phosphate transport associated with accumulation of calcium phosphate crystals within the alveolar airspaces of the lung. PAM was first described by Malpighi [1] in 1686 and was named by Puhr [2] in 1933. More than 1000 cases have been reported worldwide [3]. The disease is often discovered incidentally in asymptomatic subjects and tends to progress slowly, often resulting in respiratory insufficiency in middle age. Attempts to treat PAM empirically have been uniformly disappointing, and lung transplantation remains the only remedy for end-stage disease. The discovery that mutations in the sodium phosphate co-transporter gene SLC34A2 cause PAM has shed new light on disease pathogenesis and suggested new approaches to trials.

Epidemiology

PAM has been reported on almost every continent. The majority of cases in the literature have been from Asia (56.3%) and Europe (27.8%) [3]. The incidence per million persons is roughly 1.85 for Turkey, 1.08

Previous articles in the series: No. 1: Weatherald J, Dorfmüller P, Perros F, *et al*. Pulmonary capillary haemangiomatosis: a distinct entity? *Eur Respir Rev* 2020; 29: 190168. **No. 2:** Elia D, Torre O, Cassandro R, *et al*. Ultra-rare cystic disease. *Eur Respir Rev* 2020; 29: 190168.

Provenance: Commissioned article, peer reviewed.

Received: 25 Feb 2020 | Accepted after revision: 7 July 2020

for Italy, 0.92 for Japan, 0.15 for USA, 0.10 for China and 0.06 for India. In the literature, approximately 50% of patients are male and 41% are female, with sex being unspecified in 9% of cases. The diagnosis is most commonly made in the second through fourth decades and has been reported in persons of all ages from infants to octogenarians [4–7].

Sporadic mutations are found in about two-thirds of cases. In the report by Castellana [3], 163 families were identified with PAM accounting for 381 (37%) out of 1022 patients. In almost all familial cases, transmission was horizontal, which supports an autosomal recessive pattern of inheritance. Interestingly when three or more siblings were affected, they were usually females. In the few cases in which vertical transmission occurred, consanguinity was present. The parents were third cousins in 36 (22% of the total familial inheritance) out of 163 families and six (17%) of these 36 families exhibited vertical transmission.

Pathogenesis

The *SLC34A2* gene was identified in a DNA segment on chromosome 4p15 containing the sodium phosphate co-transporter by a Japanese group performing genome-wide high-density single-nucleotide polymorphism-based homozygosity mapping in six patients from five families [8]. Five nonrelated individuals with PAM were found to have loss of function homozygous mutations within this gene. Another independent group also implicated chromosome 4p15 through linkage analysis of a large consanguineous family with three affected members [9]. The *SLC34A2* gene comprises 13 exons of which 12 encode the type II sodium-dependent co-transporter called NPT2b (also known as NPTIIb or NaPi-IIb).

NPT2b is most abundantly expressed in the lung and small intestine, with the highest levels of expression in the alveolar epithelium and ileal epithelium, respectively, but the gene is also expressed in thyroid, salivary gland, mammary gland, uterus and testes. It is important to note that NPT2b expression in the kidney is low. In the lung, expression appears to be most abundant in alveolar type II cells, where it is thought to be required for export of phosphate generated by alveolar macrophage-mediated catabolism of surfactant phospholipids. In the gut, NPT2b functions to absorb nutritional phosphate [10]. The absence of NPT2b intestinal expression does not result in hypophosphataemia as compensatory renal mechanisms are able to maintain phosphate homeostasis in the setting of typical dietary intake of phosphate. However, mouse models suggest that when dietary phosphate is limited, NPT2b protects the host from hypophosphataemia [11]. Other genes that encode sodium phosphate cotransporters include *SLC34A1*, *SLC34A3*, *SLC20A1* and *SLC20A2*, which are also known as NPT2a, NPT2c, PIT1 and PIT2, respectively [12–14].

To date, 27 mutations have been identified that have been linked with the phenotypic development of PAM as listed in table 1 [8, 9, 15–26]. In the majority of patients with PAM who have undergone genotyping, homozygous mutations in *SLC34A2* have been identified. Compound heterozygous mutations have been described in a few patients who do not have related parents [19, 23]. Family pedigrees have demonstrated that subjects with both *SLC34A2* genes affected will almost always manifest the disease, consistent with complete penetrance [17, 18, 21].

Saito *et al.* [11] developed a murine model for PAM by deleting NPT2b in the epithelium of the lung and gut. These mice develop age-dependent radiographic manifestations of diffuse, hyperdense opacification with ground-glass infiltrates, reticular and micronodular calcific opacities and high-density consolidation with air bronchograms. Surfactant protein (SP)-D and monocyte chemoattractant protein (MCP)-1 levels are elevated in the serum of the $Npt2b^{-/-}$ animals compared to the $Npt2b^{+/+}$ mice and increase as the microlith burden progresses. When microliths from $Npt2b^{-/-}$ mice were instilled into the lungs of $Npt2b^{+/+}$ mice, histological analyses demonstrated that they were distributed throughout the lung on day 1, gathered into macrophage-rich aggregates by day 7 and completely cleared without residual inflammation or fibrosis at 1 month. The serum level of MCP-1 after microlith challenge in $Npt2b^{+/+}$ mice followed the same time course, peaking on day 7 and returning to baseline by day 28, suggesting potential utility as a biomarker of stone burden and clearance. Collectively, these data suggest that genetic correction of airway epithelial cell expression of NPT2b may be a promising future approach for reducing microlith burden in PAM. Other treatment strategies that were explored on this pre-clinical platform included low-phosphate diet treatment for 8 weeks, which effectively prevented and reversed microlith accumulation, and therapeutic alveolar lavage with calcium chelators ethylenediaminetetraacetic acid or egtazic acid, which reduced stone burden in a human PAM lung explant and $NPT2b^{-/-}$ mice.

Signs and symptoms

There is significant heterogeneity in disease onset, symptoms and natural course of disease in patients with PAM. This disease affects people of all ages and most individuals are asymptomatic in the early stages.

TABLE 1 Pathogenetic mutations

Exon	Sequence involved	Defect	First author [ref.]
1–13	195 kb deletion	Truncation without synthesis (deletion)	Stokman [15]
1	c.-6773_-6588del	Truncation without synthesis (deletion)	Corut [9]
2–6	5.5 kb deletion	Truncation (deletion)	Ishihara [16]
2	insT (not specified area)	Truncation (frameshift)	Dogan [17]
3	c.114delA	Truncation (deletion)	Corut [9]
3	c.212_224del	Truncation (deletion)	Vismara [18]
3	c.226 C>T	Substitution	Corut [9]
4	c.316 G>A	Substitution (missense)	Jonsson [19]
5	c.IVS4+1452_IVS5+660del	Truncation (deletion) of entire exon 5	Dandan [20]
6	c.560 G>A	Substitution (missense)	Jonsson [19]
6	c.575 C>A	Substitution	Ma [21]
7	c.560 G>A	Substitution (nonsense)	Jonsson [19]
7	insdel857-871	Insertion/deletion with truncation	Huqun [8]
8	IVS8+1 G>A	Truncation by splicing failure	Huqun [8]
8	c.906 G>A	Substitution (nonsense)	Jonsson [19]
8	c.910 A>T	Truncation	Zhong [22]
10	c.1136 G>A	Substitution (missense)	Jonsson [19]
11	c.1238 G>A	Substitution (nonsense)	Jonsson [19]
11	c.1327delC	Truncation (deletion)	Jonsson [19]
11	c.1328delT	Truncation (deletion)	Corut [9]
12	c.1333+1 G>A	Substitution (nonsense, frameshift splicing)	Jonsson [19]
12	c.1342delG	Truncation (deletion)	Corut [9]
12	c.1363 T>C	Substitution	Wang [23]
12	c.1390 G>C	Unclear result	Izumi [24]
12	c.1393-1404delACC	Truncation, threonine deletion	Jonsson [25]
12	c.1402-1404delACC	Truncation, threonine deletion	Jonsson [25]
12	c.1456 C>T	Truncation	Proesmans [26]

The incidental discovery of hyperdense infiltrates on chest radiographs obtained for unrelated complaints is the primary mode of presentation for PAM. It is often difficult to determine the timing of disease onset with accuracy as most patients do not have a prior chest radiograph for comparison and the natural history of the disease is unclear because of the paucity of available longitudinal studies. In the worldwide literature review of 1022 patients, a prior normal chest radiograph was available in only six (0.5%) cases and only 52 (5%) patients were followed-up for 10 years or more [3]. Even within families of affected individuals, disease course varies widely. As an example, in a family of two affected children, the younger sibling required lung transplantation, while his sister manifested only mild disease [27].

Rarely, PAM has been reported in newborns and infants, but is more typically discovered in young adulthood. Patients develop dyspnoea on exertion and dry cough as the disease progresses, but these symptoms are often less pronounced than chest radiographs would suggest, a phenomenon that has been called clinical–radiological dissociation. Additional less-common symptoms may include chest pain, cyanosis and haemoptysis. Children <5 years old have more frequent manifestations of dry cough and acute respiratory failure, with radiographic findings that differ from adult disease in that ground-glass opacities are more prominent and calcifications are often milder [28]. There are no clinical features that are known to be associated with future disease progression or useful predictive biomarkers. Although PAM is typically progressive, there are many exceptions, including reported cases in which a patient diagnosed prior to the age of 10 years lived for >45 years [29] and a man who survived for 58 years without evidence of clinical, functional or radiographic progression [30].

Pneumothorax is rare in PAM; one large review reported occurrence in 1.6% of patients [3]. There is some evidence that patients with PAM who develop pneumothorax may not respond to routine chest tube management and may require more aggressive pleural interventions such as talc pleurodesis or pleurectomy for resolution [31, 32]. One patient with a 17 pack-year smoking history had three recurrences requiring pleurectomy and stapling of apical blebs [33]. Another PAM patient underwent single lung transplantation of the hemithorax affected by recurrent pneumothorax and had residual pneumothorax at the time of transplantation [34].

Pulmonary hypertension and pulmonary fibrosis may develop over time [32]. Many patients who undergo evaluation for lung transplantation have clinical and echocardiographic evidence of pulmonary

hypertension, probably secondary to advanced pulmonary parenchymal disease with hypoxia and destruction of the pulmonary capillary bed [33, 35, 36].

Pulmonary function tests

Although pulmonary function tests (PFTs) are often normal in early disease, a restrictive defect with a reduction in diffusion capacity for carbon monoxide is most typical [37]. There are reports of asymptomatic children with radiographic findings suggestive of PAM and normal initial PFTs who develop a restrictive defect on spirometry as they enter their teenage years and further progress as they age [32]. 6-minute walk testing may demonstrate reduced exercise capacity and exercise-induced desaturation before resting hypoxia becomes evident.

Diagnostics

Serological testing

Routine blood tests are typically normal in patients with PAM. These include serum calcium and phosphorus concentrations, renal and hepatic panels, and parathyroid hormone levels [7]. Cholecalciferol (vitamin D3) levels also appear to be normal. Surfactant protein (SP)-D, produced exclusively in the lungs by club cells and alveolar type II cells [38], is elevated in the serum of patients with PAM compared to healthy volunteers and further increases with progression of illness [7, 11]. SP-D can be elevated in the serum of patients with idiopathic pulmonary fibrosis (IPF) and pulmonary alveolar proteinosis (PAP), with increased values suggestive of progressive disease [39]. The mechanisms for increased surfactant protein levels in the serum of patients afflicted by these two diseases are thought to be different; loss of integrity of the air–liquid barrier resulting in protein "leak" into the bloodstream in IPF *versus* overproduction of surfactant proteins in PAP. SP-A and SP-D levels were decreased in bronchoalveolar lavage (BAL) samples from a single case of PAM when compared to healthy volunteers [7]. Saito *et al.* [11] recently reported that MCP-1 is another potential biomarker based on mouse models. Although MCP-1 and SP-D may ultimately prove to be helpful for assessing disease severity in patients with PAM, they will not likely have diagnostic utility as they can be elevated in other pulmonary diseases.

Genetic testing

Genetic testing on DNA from peripheral blood myeloid cells that demonstrates damaging mutations in *SLC34A2* is highly specific for PAM, with at least 27 known mutations reported to date. It can accurately rule in the diagnosis for patients without the need for more invasive studies such as lung biopsy. A limited number of commercial entities offer whole-exome sequencing for the diagnosis of PAM.

Radiology

Chest radiography

Abnormal chest radiographs are often the first study suggesting PAM. Cases have been described in which an initial chest radiograph was normal and the patient went on to develop abnormal imaging [40]. The degree of microlith deposition may eventually become dense enough to produce a fine, sand-like micronodular pattern on the chest radiograph, which is often more prominent in the bases than in the apices as displayed in figure 1a. As the disease progresses, the density of the lung parenchyma may obscure the cardiac borders, diaphragms, costophrenic sinuses and cardiophrenic sulci resulting in the radiographic manifestation described as the "vanishing heart phenomenon."

High-resolution computed tomography of the chest

Computed tomography of the chest is the most useful radiologic modality for the diagnosis of PAM. Images typically reveal diffuse hyperdense micronodular airspace opaities that are most extensive in posterior segments of the lower lobes and anterior segments of the upper lobes [41]. Aggregates of microliths may manifest as calcific deposits >3mm in diameter. Ground-glass opacities may also be present, probably due to an active inflammatory reaction to intra-alveolar microliths. Parenchymal involvement may include features associated with interstitial lung disease such as subpleural interstitial thickening, interlobular septal thickening and other manifestations of pulmonary fibrosis, including subpleural reticular change and traction bronchiectasis of the peripheral airways [7, 41, 42]. Many of these features are demonstrated in figure 1b and c. The radiographic pattern of interlobular septal thickening known as "crazy-paving" may be seen in PAM, although on mediastinal windows the calcifications are seen tracing septal lines, which can help distinguish this process from PAP [43]. This can be seen in figure 1d. Progressive subpleural interstitial thickening may lead to pleural calcification, although it is rarely seen on initial diagnostic imaging [41]. Paraseptal and subpleural emphysema may manifest as regions of low attenuation adjacent to the pleural surface manifesting as small cysts.

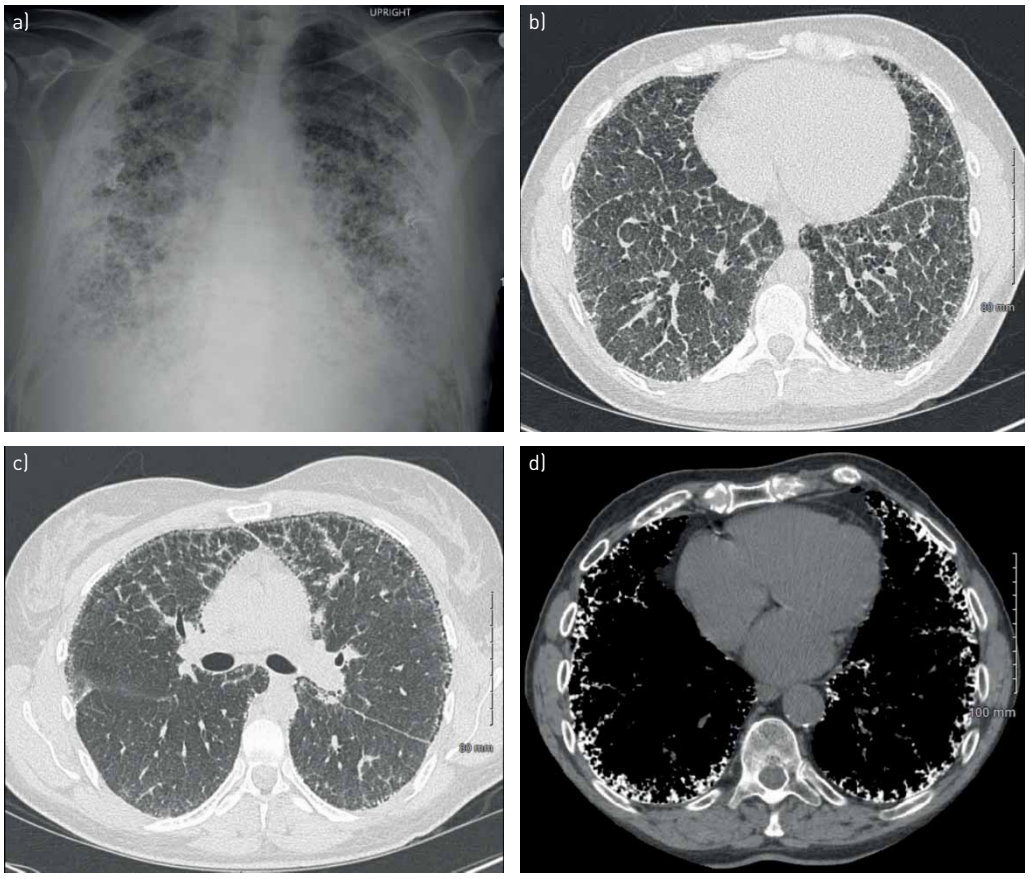

FIGURE 1 Radiographic findings in pulmonary alveolar microlithiasis. a) Chest radiograph depicting a fine, sand-like micronodular pattern with basilar predominance. b, c) High-resolution computed tomography with posterior lower lobe and anterior upper lobe micronodules, interlobular septal thickening, subpleural emphysema with predominance of small cysts. d) Mediastinal windows reveal calcific burden in the parenchyma and most concentrated in a peripheral septopleural location.

A radiographical evolution through four phases has been proposed [44]. The first (pre-calcific) phase involves a small number of poorly calcified microliths and diffuse ground-glass opacity. This presentation has been described in asymptomatic children and it is unclear whether it occurs in adults. In the second phase, the radiograph has a "sandy" appearance with scattered calcified micronodules of diameters varying between 2 and 4 mm and preserved cardiac and diaphragmatic borders. In the third phase, progressive opacification with thickening of the interstitium and obscuration of the heart and diaphragm occur. The fourth and final phase is characterised by intense calcification of the interstices with variable involvement of pleural serosa producing a "white out" appearance of the lung, sometimes with apical sparing. This may progress to areas of dense calcifiation/opacification [45]. Progression of these findings on high-resolution computed tomography (HRCT) correlates well with reductions in pulmonary function, including spirometric indices (forced expiratory volume in 1 s/forced vital capacity ratio) and diffusing capacity [41].

A black pleural line between the rib cage and calcified pulmonary infiltrate on chest radiography was first described by Felson [46]. On HRCT, it can be seen as a layer of subtle cystic changes in the subpleural ventral region or as a fat-density layer ~1–2 mm in width between the ribs and calcified parenchyma in the lower and middle lung fields [47, 48]. Use of quantitative computed tomography to assess change in mean lung density based on Hounsfield units may be useful for determining progression of disease [49].

Positron emission tomography scan

Fluorodeoxyglucose positron emission tomography was performed on an adult case revealing a maximum standardised uptake value of 7.3 in areas without calcification and lower standardised uptake value of 2.6 in areas with dense calcification [50]. This pattern suggests the presence of inflammation, especially in areas of the lung that are not yet fully calcified.

Bone scan

Early studies often utilised bone scintigraphy (technetium 99m-methylene diphosphonate bone scan) as a diagnostic test to demonstrate that opacities in the lung on chest radiography were avid for the tracer and consistent with bone [51–54]. HRCT has obviated the need for bone scintigraphy as a diagnostic modality in PAM in most cases.

Ultrasonography

Chest ultrasonography may reveal pleural thickening and irregularities as well as echogenic foci on the order of millimeters without acoustic shadowing in the subpleural area [47, 55]. The absence of expected acoustic shadow artefact (also described as the "comet tail" phenomenon) is attributed to the complex pleural interface with thickened pleura, subpleural microcysts and thickened interstitium that may reduce deep penetration of ultrasound waves.

Pathology

Lung tissues may be obtained by transbronchial forceps biopsy, transbronchial cryobiopsy, surgical lung biopsy, as lung explants from transplanted patients or at autopsy. Gross anatomical analysis of explanted lung tissue reveals a granular and nodular pleural surface with fibrous and calcified areas [56]. Cut sections of the lung have a granular consistency due to extensive round or ovoid microcalcifications that may be accentuated along interlobular septa (figure 2a–c) [37]. Variably sized concentrically laminated concretions are present both in alveolar spaces and in the interstitium with diameters ranging from 0.01 to 2.8 mm (figure 2d and e) [37]. The microliths contain calcium which can be highlighted on histologic

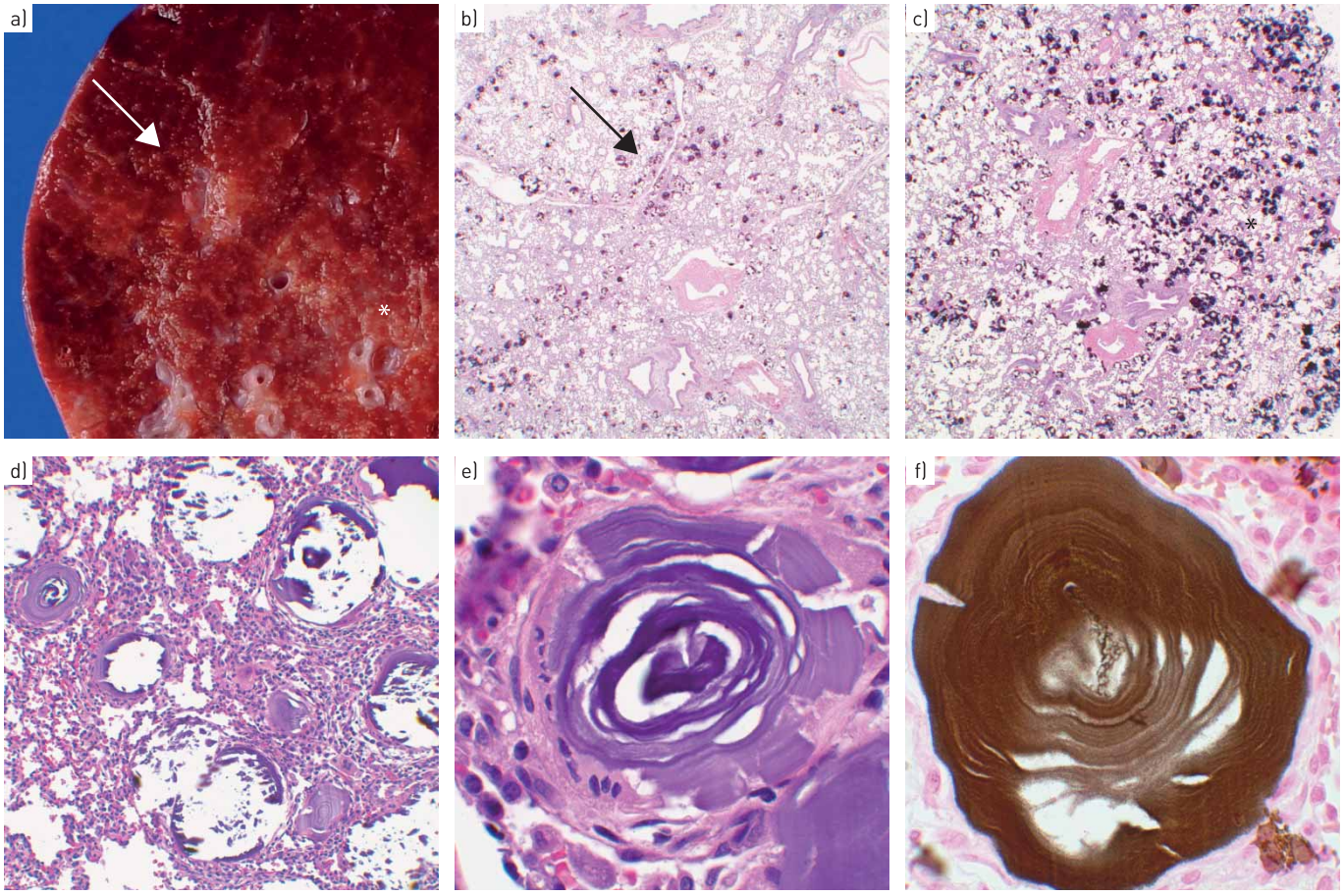

FIGURE 2 Pathologic findings in pulmonary alveolar microlithiasis (PAM). a) Lung explant from a 2-year-old boy transplanted for PAM showing lung regions with accentuation of the interlobular septa by microlith accumulations (arrow) and other regions with more diffuse accumulations of granular, gritty microliths (*). b, c) Histological sections showing microliths along interlobular septa (b, arrow) and areas with more diffuse microlith accumulations (c). d) Varying sized microliths are present both in the alveolar spaces and interstitium. e) The microliths are characteristically concentrically laminated calcified spherules. f) Calcium can be demonstrated in the microliths by Von Kossa stain. b–e) Haematoxylin and eosin stain; original magnifications ×20 (b, c), ×200 (d), ×1000 (e, f).

sections with a Von Kossa stain (figure 2f). Progression of parenchymal disease can result in cicatricial fibrosis with foci of metastatic ossification [57].

Cytologic and sputum studies

Microliths may be seen in expectorated sputum or BAL samples, and can be used to establish a definitive diagnosis in the setting of a typical history and HRCT. Microliths in expectorated sputum are not entirely specific for PAM and may occasionally be seen in patients with COPD and lung cancer [58, 59]. Histology demonstrating the typical lamellar structure of microliths can help to distinguish them from other airway calculi in the differential. Although Curschmann's spirals, associated with asthma and chronic bronchitis, are composed of glycoproteins and are not typically calcified, patients with PAM may develop a bronchial mold with calcifications that have a similar appearance that is distinct from the classic lamellar calcified bodies that are typical of microliths [58, 60–62]. Psammoma bodies are concentric calcified laminated structures that form within epithelial cell aggregates or small tissue fragments and are often associated with adenocarcinoma [45, 59, 63–65].

Scanning electron microscopy

Scanning electron microscopy (SEM) can demonstrate the spherical structure of microliths with a typical porous surface reminiscent of cortical bone. The elemental structure has been determined using energy-dispersive X-ray diffraction analyses, which typically reveal calcium and phosphorus salts with traces of metals such as iron, copper and magnesium [66]. The ratio of calcium to phosphate is approximately 2:1 to 3:1, consistent with the composition of hydroxyapatite [67]. SEM has been used to characterise particulate matter in BAL samples from pneumoconiosis populations, including silicosis and asbestosis [68–70]. SEM images and energy-dispersive spectroscopy (EDAX) obtained in PAM patients are displayed in figure 3. Demonstrating the characteristic structure and elemental composition of BAL microliths by SEM and EDAX has potential as a noninvasive diagnostic approach for PAM.

Extrapulmonary manifestations

Multiple case reports have described the potential association of calcifications in the genitalia of male patients with PAM, including microliths within the testes, seminal vesicles, epididymis and sympathetic ganglia, a condition called testicular microlithiasis. Testicular microlithiasis has a prevalence of 0.6–0.9% in the general male population, can be associated with up to 1% of all idiopathic infertility cases and has been linked to testicular malignancies [9]. Testicular microlithiasis can lead to bilateral testicular atrophy and obstructive azoospermia [71–76]. Presenting symptoms include recurrent abdominal pain, recurrent haematuria and infertility. Affected patients typically present in the third and fourth decades. Corut *et al.* [9] evaluated 15 subjects with diffuse bilateral testicular microlithiasis and identified two patients with heterozygous mutations in *SLC34A2*, although it was unclear whether these rare mutations were damaging. They also found no evidence of testicular microlithiasis in seven male subjects with known PAM from this group. It remains unclear whether these were chance associations or whether testicular microlithiasis is a manifestation of PAM.

Finger clubbing (also known as secondary hypertrophic pulmonary osteoarthropathy) is typically present in advanced stages of PAM, seen in 7% of the worldwide 1022 cases reviewed [3]. It can also be seen in mild presentations of symptomatic disease [77]. Increased radioisotope bone scan uptake has been reported at the diaphysis and metaphysis of metacarpal bones and wrists [42].

Comorbidities

In a large review, diseases reported to be associated with PAM included rheumatoid arthritis, Sjögren syndrome, lymphocytic interstitial pneumonitis, psoriasis, antiphospholipid syndrome and discoid lupus after varicella zoster infection, diaphyseal aclasia, autosomal recessive Waardenburg-anophthalmia, milk alkali syndrome, pericardial cyst, osteopetrosis, pectus excavatum and non-Hodgkin lymphoma [3]. The prevalence of each of these comorbid diseases in PAM is very low and a direct association with the disease is conjecture at best.

Diagnosis

Although a clinically confident diagnosis of PAM can often be made based on radiographic studies, a definitive diagnosis requires at least one additional clinical feature including microlith analysis (recovered in sputum or BAL), histopathology, a positive family history or genetic testing demonstrating a mutation in *SLC34A2*. An algorithm for the diagnosis has been proposed that employs a progression from the least invasive to most invasive analyses in step-wise fashion (figure 4). PAM is often initially suspected when a compatible radiograph is obtained in a patient who presents for employment screening, unrelated complaints or respiratory symptoms of dyspnoea or cough [44]. If there is a family history of an affected

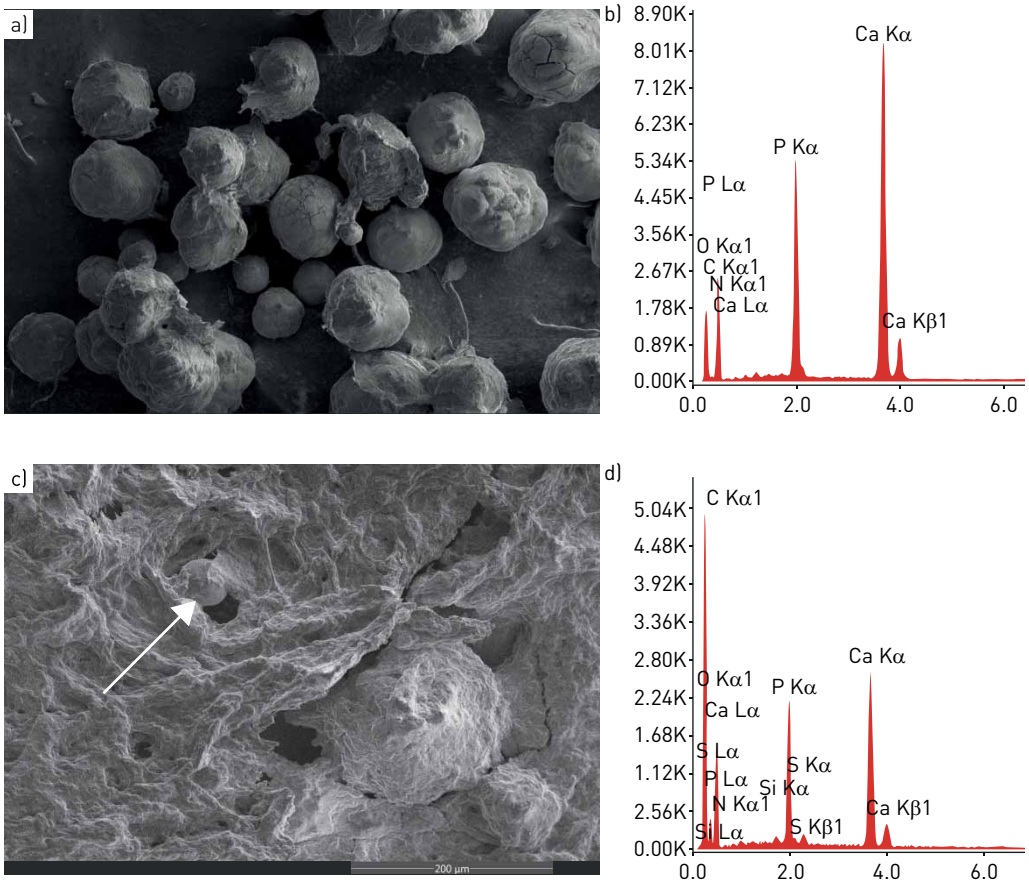

FIGURE 3 Scanning electron microscopy (SEM) and energy-dispersive spectroscopy (EDAX) of pulmonary alveolar microlithiasis (PAM). a, b) Microliths isolated from explanted lungs demonstrating a) the characteristic spherical structure and b) inorganic elemental signature. Microlith (white arrow) in bronchoalveolar lavage (BAL) fluid with SEM (c) and EDAX characteristics that are similar to explant controls, demonstrating feasibility of using SEM and EDAX as a diagnostic BAL test for PAM. Note carbon spike associated with debris from lavage. Kα, Kβ and Lα represent X-rays emitted as electrons return to K and/or L electron shell. d) Inorganic elemental analysis of BAL microliths.

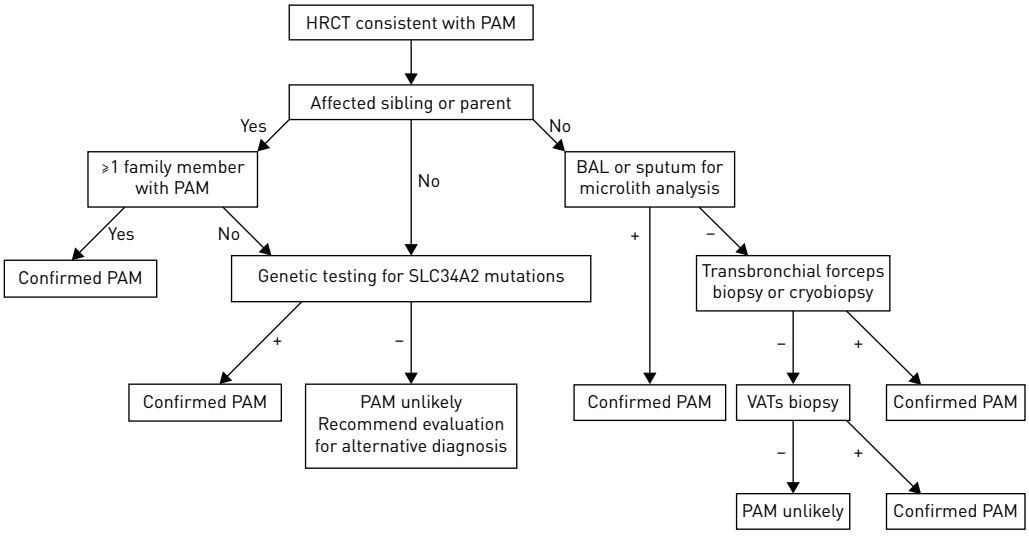

FIGURE 4 Diagnostic algorithm for patients with suspected pulmonary alveolar microlithiasis (PAM). Obtaining a family and genetic testing history is key. Thereafter, diagnostic modalities progress from least invasive to most invasive. HRCT: high-resolution computed tomography; BAL: bronchoalveolar lavage; VAT: video-assisted thoracoscopic biopsy.

sibling or parent with positive genetic testing and chest radiograph or HRCT shows typical hyperdense mironodular air sapce opacities, the diagnosis is certain. In the absence of genetic confirmation in family members, genotyping of the index patient is the most appropriate next step if available. Sporadic mutations that occur in the absence of a known family history comprise the majority of new cases [3].

If genetic testing is unavailable, unaffordable or impractical and it is determined that diagnostic certainty is required based on patient preference, need to exclude treatable diseases in the differential diagnosis or the emergence of a therapy for PAM, examination of sputum for microliths followed by BAL with or without transbronchial biopsy are reasonable next steps. Identification of lamellar microliths in sputum or in the cell block consisting of BAL cells in the setting of a characteristic HRCT is considered to be diagnostic, although the sensitivity and specificity of these approaches is unknown. A transbronchial biopsy showing microliths within the alveolar lumen is more convincing, but yield is subject to sampling error and dependent on the extent of microlith deposition and is assoiated with risks of bleeding and pneumothorax. Transbronchial cryobiopsy is an emerging diagnostic technique that provides up to three to four times more tissue than transbronchial forceps biopsy, but is also associated with an increased risk of bleeding and pneumothorax [78, 79]. To our knowledge, cryobiopsy has not yet been attempted for the diagnosis of PAM. Video-assisted thoracoscopic biopsy is the gold standard for diagnosis but because of the risks associated with general anaesthesia and chronic pain that can follow thoracostomy, it should be reserved for cases in which less-invasive approaches have been unavailable or unsuccessful.

Differential diagnosis

Diffuse pulmonary calcifications may also be seen in miliary tuberculosis, silicosis, amyloidosis, berylliosis, sarcoidosis, lipoidal emboli, hemosiderosis, healed varicella or variola pneumonia, fungal infections including histoplasmosis and coccidioidomycosis, dendriform pulmonary ossification and metastatic calcification from hyperparathyroidism, end-stage renal disease or malignancy [80–83]. The patterns of calcifications differ in these diseases and rarely progress to obscure the heart border as can occur in PAM. The metastatic and dystrophic calcifications that occur in other PAM mimics are located in the interstitial or vascular compartments as opposed to the almost exclusive intra-alveolar calcification in PAM [84]. A few radiographic examples of these processes that can be mistaken for PAM are included in figure 5.

Tuberculosis has been mentioned in multiple case reports as having been previously treated in individuals with PAM [7, 57, 85]. The means by which diagnosis had been made at time of treatment is unclear, but it is likely that the early radiographic appearance of PAM may have prompted the diagnosis of tuberculosis without microbiological confirmation in prevalent populations where the two diseases overlap. Out of 13 patients initially diagnosed with miliary tuberculosis in a Turkish case series, two (15%) patients were found to have positive Acid fast bacilli smears [86], but it is unclear how many in that cohort were empirically treated for tuberculosis. An additional patient who underwent lung transplantation had been

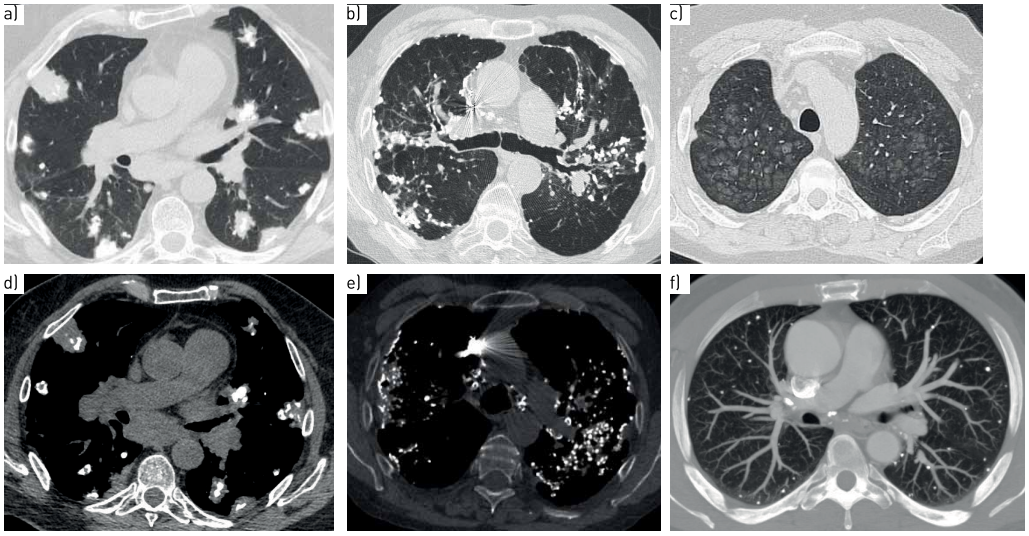

FIGURE 5 Other examples of diffuse lung calcification. Computed tomography depicting examples of a, d) amyloidosis with calcified masses, lymphadenopathy and rare cysts, b, e) silicosis with peri-lymphatic calcified nodules, eggshell lymph node calcifications and conglomerate fibrosis, c) metastatic pulmonary calcification in chronic renal failure characterised by lobular ground-glass opacity with interlobular septal sparing and f) healed granulomas due to histoplasmosis with maximum intensity projection reformats.

previously treated with anti-tuberculosis therapy for 18 months despite negative smears, cultures and a nonreactive purified protein derivative [87].

Pharmacological treatment options

Given the absence of any organised trials to assess the safety and efficacy of pharmacological therapies in PAM, all available data are derived from case reports of empiric therapies in small numbers of patients.

Bisphosphonates

Bisphosphonates adsorb onto bones rendering them resistant to osteoclast-mediated resorption by inhibiting the development, function and viability of osteoclasts. Compared to more frequently used bisphosphonates such as alendronate and risedronate, disodium etidronate is less potent as an anti-osteoclast agent but has the unique theoretical benefit in PAM that it inhibits hydroxyapatite crystal formation [88].

Etidronate treatment has been reported to benefit children with PAM. In one case, a 3.5-year-old girl with PAM, failure to thrive and nonproductive cough had radiographic and symptomatic improvement after 36 months of daily oral disodium etidronate [89]. She continued disodium etidronate for a total of 9 years, and then was conservatively managed without intervention for 11 years [90]. At the end of the observation period, PFTs revealed a nonsignificant decrease in spirometric indices and minimal progression of septal thickening and calcifications on HRCT compared to her baseline. Similarly, a 9-year-old girl with failure to thrive, who was found to have radiographs compatible with PAM, exhibited radiographic improvement on HRCT after 12 months of treatment with oral disodium etidronate [91]. Her schedule of disodium etidronate administration was modified after she developed rickets as a complication of therapy. She continued on a 15-day cycle of disodium etidronate treatment every 4 months for 11 years of total therapy with documented improvement in spirometry [90]. Finally, an 11-year-old boy and his twin 4-year-old sisters with the same homozygous *SLC34A2* gene mutation were treated with disodium etidronate. The boy and one of his female siblings had improvement in radiographic chest radiography and HRCT findings after 12 months of treatment with disodium etidronate [92], but the other twin did not show any improvement. These data indicate that even in patients with the same genetic defect, there can be considerable variability in treatment response.

Adverse effects of bisphosphonate therapy include transient hypocalcaemia, osteomalacia, transient fevers, ocular complications, transient myalgia, leukopenia, lymphopenia and widening of the growth plate in children, resulting in rickets [93].

There have also been cases in the literature in which treatment with bisphosphonates was unsuccessful. An 8.5-year-old girl with lung biopsy-proven PAM and normal PFTs underwent 18 months of treatment with daily disodium etidronate without radiographic improvement in chest radiography although no repeat PFTs or HRCT were performed [94]. There have not been any published examples of benefit of bisphosphonate therapy in adults, although it is unclear whether the duration of therapy was adequate in those cases. A 46-year-old man with biopsy-proven PAM and fibrotic damage underwent sodium etidronate oral therapy for 6 months without improvement on chest radiography, although symptoms remained stable [95]. In a small case series, two patients were treated for a duration of 6 months and 1.5 years respectively with continued progression of their lung disease [19]. Disodium etidronate treatment was attempted in an 18-year-old and 51-year-old man who did not symptomatically benefit after 2 years and 6 months of therapy, respectively and who self-discontinued therapy [25]. Weekly alendronate was administered over 6 and 12 months to two adult men in their fifth decade with symptomatic improvement, although radiographs were unchanged [96].

Inhaled corticosteroids

Inhaled corticosteroid therapy does not appear to improve radiographical manifestations of PAM. It has been used effectively to treat symptoms and abnormal lung function in PAM patients who present with accompanying conditions such as spirometrically proven obstructive lung disease suggestive of asthma, lymphocytic interstitial pneumonitis and discoid lupus erythematosus among others [97–99], but there is little evidence to support routine inhaled corticosteroid use in patients with PAM.

Systemic corticosteroids

A few clinicians have trialed systemic corticosteroids as a treatment option for PAM. Badger *et al.* [100] provided steroid treatment for 48 days in a PAM patient without improvement. In one review, two patients were treated with prednisone; the first was a 66-year-old and was lost to follow-up, and the second was an adult who was treated for 2 months without effect [19]. Prior to transplantation, a 47-year-old man who

underwent treatment with prednisone was said to have experienced partial improvement, although it is unclear how this was measured [57].

Sodium thiosulfate

Sodium thiosulfate (STS) is a calcium-chelating and solubilising agent that has been employed to treat diseases associated with heterotopic ossification such as calciphylaxis in end-stage renal disease [101]. Both systemic therapy and direct intra-lesional injection have been reported to be effective and since trials are lacking, treatment remains empiric at this time [102]. Taille *et al.* [49] attempted a less intensive monthly intravenous infusion over 9 months without improvement in symptoms, PFTs or microlith burden per HRCT evaluation. Instead, they observed a marked increase in lung density as well as decreased diffusion and postulated that the STS dose or interval used may have been inadequate to inhibit disease progression. It is also possible that the STS treatment accelerated disease progression.

Low-phosphate diet

Treatment of *Npt2b*$^{-/-}$ mice with marked dietary phosphate restriction results in prevention of microlith accumulation and reduction in microlith burden, perhaps through upregulation of alternative alveolar phosphate transporters and/or pulmonary osteoclast activity [11]. An adult patient who was treated with a low-phosphate diet for 2 years with reduction in serum phosphate experienced continued progression of lung disease [19]. One possible explanation for the failure of diet to affect microlith burden in affected individuals is that the level of dietary phosphate restriction that is practical in humans (from an average daily intake of approximately 1.8 g·day^{-1} to about 1 g·day^{-1}) is less than a two-fold reduction, compared to the 5–7-fold reduction that was shown to produce a beneficial effect on microlith burden in mice. Trials are needed before recommendations are made to restrict dietary phosphate intake, but until they are performed it may be prudent for PAM patients to avoid foods with very high phosphate content such as fizzy drinks and processed cheeses and meats.

Supportive management

Although there are no PAM studies suggesting an improvement in mortality, exercise tolerance or quality of life with oxygen therapy, recommendations have been made to ensure a resting and exertional oxygen goal of ⩾88% in patients without cor pulmonale and >90% in those with cor pulmonale [103]. In one case, a nonobese patient with cor pulmonale had reduced shunt fraction and improved daytime oxygenation after use of nocturnal continuous positive airway pressure with sustained improvement in exercise tolerance 3 months after initiation [104]. Similarly, patients with PAM should obtain routine vaccinations for influenza and *Pneumococcus* and be encouraged to stop smoking cigarettes, as is appropriate for all individuals with chronic lung disease.

Procedural/surgical treatment options

Whole lung lavage

Whole lung lavage has been attempted by a few investigators to determine whether microliths could be removed manually. Although abundant spherules of ⩽1 mm were recovered in the serial lavages in a single patient, there was no significant change in radiographical abnormalities [105]. In another case, lavage with 22 L of buffered saline was successful in removing 14.5 g of solid material, but without improvement in radiographic findings or clinical symptoms [32]. The investigators postulated that microliths exceeding the diameter of the alveolar orifice or respiratory bronchioles could not be easily removed by whole lung lavage.

Lung transplantation

The only proven treatment for advanced PAM is lung transplantation. Despite multiple procedural challenges, including calcified lung parenchyma limiting intra-operative deflation and access to the hilum, more dense pleural adhesions and a higher risk of intra-operative and post-operative bleeding, both single lung and double lung transplantation have been successful in PAM (table 2) [27, 33–36, 57, 87, 106–113]. There were some initial concerns that pulmonary shunting might compromise outcomes in single lung transplantation, but this has proven to be unfounded. To date there have not been any documented recurrences of intra-alveolar microliths in lung transplant patients.

In a small case series of PAM patients from the Medical University of Vienna (Vienna, Austria), all five patients underwent bilateral lung transplantation with a mean age of 46.3 years [35]. The mean interval from the onset of symptoms to transplantation was 8.6 years, and the majority of patients were found to have secondary pulmonary hypertension at presentation. In the post-operative period, one patient had primary graft dysfunction with re-transplantation on post-operative day two and then subsequently died from sepsis on post-operative day 11. The remaining four patients did well without recurrence of

TABLE 2 Lung transplantation in cases of pulmonary alveolar microlithiasis

Single *versus* double	Age at transplant years	Sex	Outcome	Complication(s)	First author [ref.]
Single	32	Male	Death, NR	PGD, haemodynamic instability	Shadmehr [106]
Single	47	Female	Alive, 12 months	Possible acute rejection, bronchial stricture	Raffa [87]
Single	53	Male	Alive, 12 months	Bronchial anastomosis granulation with stenosis, bacterial infection	Ren [34]
Single	53	Female	Alive, 90 months	None	Jackson [107]
Single	64	Female	Alive, 60 months	None	Borrelli [108]
Double	32	Female	Death, 11 days	PGD, sepsis	Klikovits [35]
Double	32	Male	Alive, 18 months	Bronchial artery bleed, post-operative tracheostomy, CMV/fungal infections	Stamatis [27]
Double	34	Male	Alive, 67 months	None	Klikovits [35]
Double	36	Female	Alive, 32 months	None	Edelman [33]
Double	45	Male	Alive, 12 months	Mild PGD	Alrossais [36]
Double	46	Female	Death, 20 months	Bronchiolitis obliterans	Bonnette [109]
Double	48	Male	Alive, 12 months	PGD, haemodynamic instability, ARF	Samano [57]
Double	49	Female	Death, 3 months	Infection	Coulibaly [110]
Double	52	Female	Alive, 35 months	None	Klikovits [35]
Double	52	Female	Alive, 74 months	PGD, atrial fibrillation	Klikovits [35]
Double	53	Female	Alive, 12 months	None	Gucyetmez [111]
Double	54	Female	Alive, 12 months	None	Jindal [112]
Double	56	Male	Death, 5 days	Post-operative bleeding	Edelman [33]
Double	62	Female	Alive, 29 months	Atrial fibrillation	Klikovits [35]
Double	63	Female	Alive, 24 months	None	Shigemura [113]

NR: not reported; PGD: primary graft dysfunction; CMV: cytomegalovirus; ARF: acute renal failure.

intra-alveolar microliths up to 74 months from transplantation. The survival of patients in this PAM cohort was comparable to those undergoing lung transplantation for other indications.

Prognosis

There are few longitudinal studies that can be used to inform prognosis in patients with PAM. In a long-term follow-up study of 53 Japanese patients, respiratory insufficiency was the cause of death in 34.1% of patients within 10–20 years of diagnosis, and of those surviving, an additional 42.9% within 20–49 years of diagnosis [114]. Mean survival overall was to an age of 46.2 years.

Future directions

PAM is a fascinating disease in which the lung fills with bone-like alveolar calculi and results in slowly progressive respiratory failure. There are no effective treatments and management is largely supportive with lung transplantation reserved for those with progressive disease. The discovery of the genetic basis of PAM is a major advance that sheds light on disease pathogenesis and suggests strategies for development of future biomarkers and therapies. Because of the rarity of the disease, for trials to be successful, patients with PAM must organise in a manner that facilitates research.

Conflict of interest: None declared.

Support statement: This work was supported in part by the HL127455 and the National Center for Advancing Translational Sciences (NCATS).

References

1 Malpighi M. Manoscritti, vol. XII, foglio 81. 1686.
2 Puhr L. Mikrolithiasis alveolaris pulmonum. *Virchows Arch Pathol Anat Physiol Klin Med* 1933; 290: 156–160.
3 Castellana G, Castellana G, Gentile M, *et al.* Pulmonary alveolar microlithiasis: review of the 1022 cases reported worldwide. *Eur Respir Rev* 2015; 24: 607–620.
4 Caffrey PR, Altman RS. Pulmonary alveolar microlithiasis occurring in premature twins. *J Pediatr* 1965; 66: 758–763.
5 Dahabreh M, Najada A. Pulmonary alveolar microlithiasis in an 8-month-old infant. *Ann Trop Paediatr* 2009; 29: 55–59.
6 Krishnakurup J, Abdelsayed G. The calcareous lung. *Mayo Clin Proc* 2011; 86: 85.
7 Takahashi H, Chiba H, Shiratori M, *et al.* Elevated serum surfactant protein A and D in pulmonary alveolar microlithiasis. *Respirology* 2006; 11: 330–333.
8 Huqun Izumi, S, Miyazawa H, *et al.* Mutations in the SLC34A2 gene are associated with pulmonary alveolar microlithiasis. *Am J Respir Crit Care Med* 2007; 175: 263–268.
9 Corut A, Senyigit A, Ugur SA, *et al.* Mutations in SLC34A2 cause pulmonary alveolar microlithiasis and are possibly associated with testicular microlithiasis. *Am J Hum Genet* 2006; 79: 650–656.
10 Sabbagh Y, O'Brien SP, Song W, *et al.* Intestinal NPT2b plays a major role in phosphate absorption and homeostasis. *J Am Soc Nephrol* 2009; 20: 2348–2358.
11 Saito A, Nikolaidis NM, Amlal H, *et al.* Modeling pulmonary alveolar microlithiasis by epithelial deletion of the Npt2b sodium phosphate cotransporter reveals putative biomarkers and strategies for treatment. *Sci Transl Med* 2015; 7: 313ra181.
12 Forster IC, Hernando N, Biber J, *et al.* Phosphate transporters of the SLC20 and SLC34 families. *Mol Aspects Med* 2013; 34: 386–395.
13 Biber J, Hernando N, Forster I. Phosphate transporters and their function. *Annu Rev Physiol* 2013; 75: 535–550.
14 Nishimura M, Naito S. Tissue-specific mRNA expression profiles of human solute carrier transporter superfamilies. *Drug Metab Pharmacokinet* 2008; 23: 22–44.
15 Stokman L, Nossent EJ, Grunberg K, *et al.* A case of pulmonary alveolar microlithiasis associated with a homozygous 195 kb deletion encompassing the entire SLC34A2 gene. *Clin Case Rep* 2016; 4: 412–415.
16 Ishihara Y, Hagiwara K, Zen K, *et al.* A case of pulmonary alveolar microlithiasis with an intragenetic deletion in SLC34A2 detected by a genome-wide SNP study. *Thorax* 2009; 64: 365–367.
17 Dogan OT, Ozsahin SL, Gul E, *et al.* A frame-shift mutation in the SLC34A2 gene in three patients with pulmonary alveolar microlithiasis in an inbred family. *Intern Med* 2010; 49: 45–49.
18 Vismara MF, Colao E, Fabiani F, *et al.* The sodium-phosphate co-transporter SLC34A2, and pulmonary alveolar microlithiasis: presentation of an inbred family and a novel truncating mutation in exon 3. *Respir Med Case Rep* 2015; 16: 77–80.
19 Jonsson ALM, Bendstrup E, Mogensen S, *et al.* Eight novel variants in the SLC34A2 gene in pulmonary alveolar microlithiasis. *Eur Respir J* 2020; 55: 1900806.
20 Dandan S, Yuqin C, Wei L, *et al.* Novel deletion of SLC34A2 in Chinese patients of PAM shares mutation hot spot with fusion gene SLC34A2-ROS1 in lung cancer. *J Genet* 2018; 97: 939–944.
21 Ma T, Ren J, Yin J, *et al.* A pedigree with pulmonary alveolar microlithiasis: a clinical case report and literature review. *Cell Biochem Biophys* 2014; 70: 565–572.
22 Zhong YQ, Hu CP, Cai XD, *et al.* [A novel mutation of the SLC34A2 gene in a Chinese pedigree with pulmonary alveolar microlithiasis]. *Zhonghua Yi Xue Yi Chuan Xue Za Zhi* 2009; 26: 365–368.
23 Wang H, Yin X, Wu D, *et al.* SLC34A2 gene compound heterozygous mutation identification in a patient with pulmonary alveolar microlithiasis and computational 3D protein structure prediction. *Meta Gene* 2014; 2: 557–564.
24 Izumi H, Kurai J, Kodani M, *et al.* A novel SLC34A2 mutation in a patient with pulmonary alveolar microlithiasis. *Hum Genome Var* 2017; 4: 16047.
25 Jonsson AL, Simonsen U, Hilberg O, *et al.* Pulmonary alveolar microlithiasis: two case reports and review of the literature. *Eur Respir Rev* 2012; 21: 249–256.
26 Proesmans M, Boon M, Verbeken E, *et al.* Pulmonary alveolar microlithiasis: a case report and review of the literature. *Eur J Pediatr* 2012; 171: 1069–1072.
27 Stamatis G, Zerkowski HR, Doetsch N, *et al.* Sequential bilateral lung transplantation for pulmonary alveolar microlithiasis. *Ann Thorac Surg* 1993; 56: 972–975.
28 Sigur E, Roditis L, Labouret G, *et al.* Pulmonary alveolar microlithiasis in children less than 5 years of age. *J Pediatr* 2020; 217: 158–164.
29 Jinta T, Tomishima Y, Horinouchi H, *et al.* A case of pulmonary alveolar microlithiasis in which dialysis was performed for the concomitant renal disease. *Ann Jpn Respir Soc* 2012; 1: 267–272.
30 Castellana G, Fanella C, Napoli D, *et al.* La microlitiasi alveolare polmonare: decorso clinic, terapia e rivitazione di un singolare caso lungovivente. *Quad Pat Tor D Cotugno* 1998; 7: 26–29.
31 Devine OP, Harborne AC. Pneumothorax secondary to pulmonary alveolar microlithiasis. *Clin Case Rep* 2018; 6: 764–765.
32 Mascie-Taylor BH, Wardman AG, Madden CA, *et al.* A case of alveolar microlithiasis: observation over 22 years and recovery of material by lavage. *Thorax* 1985; 40: 952–953.
33 Edelman JD, Bavaria J, Kaiser LR, *et al.* Bilateral sequential lung transplantation for pulmonary alveolar microlithiasis. *Chest* 1997; 112: 1140–1144.
34 Ren XY, Fang XM, Chen JY, *et al.* Single-lung transplantation for pulmonary alveolar microlithiasis: a case report. *World J Clin Cases* 2019; 7: 3851–3858.

35 Klikovits T, Slama A, Hoetzenecker K, *et al.* A rare indication for lung transplantation - pulmonary alveolar microlithiasis: institutional experience of five consecutive cases. *Clin Transplant* 2016; 30: 429–434.
36 Alrossais NM, Alshammari AM, Alrayes AM, *et al.* Pulmonary hypertension and polycythemia secondary to pulmonary alveolar microlithiasis treated with sequential bilateral lung transplant: a case study and literature review. *Am J Case Rep* 2019; 20: 1114–1119.
37 Prakash UB, Barham SS, Rosenow EC 3rd, *et al.* Pulmonary alveolar microlithiasis. A review including ultrastructural and pulmonary function studies. *Mayo Clin Proc* 1983; 58: 290–300.
38 Hawgood S, Clements J. Surfactant proteins A and D: disease markers. *Biochim Biophys Acta* 1990; 1408: 334–345.
39 Maher TM, Oballa E, Simpson JK, *et al.* An epithelial biomarker signature for idiopathic pulmonary fibrosis: an analysis from the multicentre PROFILE cohort study. *Lancet Respir Med* 2017; 5: 946–955.
40 Biressi PC, Casassa PM. Intra-alveolar pulmonary microlithiasis. *Minerva Med* 1956; 47: 930–939.
41 Deniz O, Ors F, Tozkoparan E, *et al.* High resolution computed tomographic features of pulmonary alveolar microlithiasis. *Eur J Radiol* 2005; 55: 452–460.
42 Emri S, Coplu L, Selcuk ZT, *et al.* Hypertrophic pulmonary osteoarthropathy in a patient with pulmonary alveolar microlithiasis. *Thorax* 1991; 46: 145–146.
43 Gasparetto EL, Tazoniero P, Escuissato DL, *et al.* Pulmonary alveolar microlithiasis presenting with crazy-paving pattern on high resolution CT. *Br J Radiol* 2004; 77: 974–976.
44 Castellana G, Castellana R, Fanelli C, *et al.* Pulmonary alveolar microlithiasis: clinical and radiological course of three cases according to conventional radiology and HRCT. A hypothesis for radiological classification. *Radiol Med* 2003; 106: 160–168.
45 Gupta PK, Mittal R, Chhabra SK. Calcified pulmonary consolidations in pulmonary alveolar microlithiasis: uncommon computed tomographic appearance of a rare disease. *Lung India* 2017; 34: 297–299.
46 Felson B. The Roentgen diagnosis of disseminated pulmonary alveolar diseases. *Semin Roentgenol* 1967; 2: 3–21.
47 Rea G, Sperandeo M, Sorrentino N, *et al.* Chest ultrasound findings in pulmonary alveolar microlithiasis. *J Med Ultrason (2001)* 2015; 42: 591–594.
48 Hoshino H, Koba H, Inomata S, *et al.* Pulmonary alveolar microlithiasis: high-resolution CT and MR findings. *J Comput Assist Tomogr* 1998; 22: 245–248.
49 Taille C, Debray MP, Danel C, *et al.* Calcium-solubilizing sodium thiosulfate failed to improve pulmonary alveolar microlithiasis: evaluation of calcium content with CT scan. *Respir Med Res* 2019; 75: 10–12.
50 Ito K, Kubota K, Yukihiro M, *et al.* FDG-PET/CT finding of high uptake in pulmonary alveolar microlithiasis. *Ann Nucl Med* 2007; 21: 415–418.
51 Sahoo MK, Karunanithi S, Bal CS. Pulmonary alveolar microlithiasis: imaging characteristics of planar and SPECT/CT bone scan *versus* 18F-FDG and 18F-sodium fluoride PET/CT scanning. *Jpn J Radiol* 2013; 31: 766–769.
52 Alkhankan E, Yamin H, Bukamur H, *et al.* Pulmonary alveolar microlithiasis diagnosed with radiography, CT, and bone scintigraphy. *Radiol Case Rep* 2019; 14: 775–777.
53 Fallahi B, Ghafary BM, Fard-Esfahani A, *et al.* Diffuse pulmonary uptake of bone-seeking radiotracer in bone scintigraphy of a rare case of pulmonary alveolar microlithiasis. *Indian J Nucl Med* 2015; 30: 277–279.
54 Arpag H, Sayan M, Atilla N, *et al.* A case of pulmonary alveolar microlithiasis diagnosed by transbronchial biopsy. *Turk Thorac J* 2017; 18: 134–136.
55 Resorlu M, Toprak CA, Aylanc N, *et al.* Ultrasonography and computed tomography findings in pulmonary alveolar microlithiasis. *Rofo* 2018; 190: 1063–1064.
56 Siddiqui NA, Fuhrman CR. Best cases from the AFIP: pulmonary alveolar microlithiasis. *Radiographics* 2011; 31: 585–590.
57 Samano MN, Waisberg DR, Canzian M, *et al.* Lung transplantation for pulmonary alveolar microlithiasis: a case report. *Clinics (Sao Paulo)* 2010; 65: 233–236.
58 Tao LC. Microliths in sputum specimens and their relationship to pulmonary alveolar microlithiasis. *Am J Clin Pathol* 1978; 69: 482–485.
59 Martinez-Giron R, Martinez-Torre S, Tamargo-Pelaez ML, *et al.* Calcareous concretions and psammoma bodies in sputum smears: do these similar structures have different clinical significance? *Diagn Cytopathol* 2014; 42: 759–765.
60 Antonakopoulos GN, Lambrinaki E, Kyrkou KA. Curschmann's spirals in sputum: histochemical evidence of bronchial gland ductal origin. *Diagn Cytopathol* 1987; 3: 291–294.
61 Sakula A. Charcot-Leyden crystals and Curschmann spirals in asthmatic sputum. *Thorax* 1986; 41: 503–507.
62 Martinez-Giron R, Martinez-Torre S. Calcified Curschmann's spirals and microliths in sputum smears from a case of pulmonary alveolar microlithiasis. *Diagn Cytopathol* 2017; 45: 1116–1118.
63 Salisbury JR, Darby AJ, Whimster WF. Papillary adenocarcinoma of lung with psammoma bodies: report of a case derived from type II pneumocytes. *Histopathology* 1986; 10: 877–884.
64 Silverman JF, Finley JL, Park HK, *et al.* Psammoma bodies and optically clear nuclei in bronchiolo-alveolar cell carcinoma. Diagnosis by fine needle aspiration biopsy with histologic and ultrastructural confirmation. *Diagn Cytopathol* 1985; 1: 205–215.
65 Chen KT. Psammoma bodies in fine-needle aspiration cytology of papillary adenocarcinoma of the lung. *Diagn Cytopathol* 1990; 6: 271–274.
66 Moran CA, Hochholzer L, Hasleton PS, *et al.* Pulmonary alveolar microlithiasis. A clinicopathologic and chemical analysis of seven cases. *Arch Pathol Lab Med* 1997; 121: 607–611.
67 Pracyk JB, Simonson SG, Young SL, *et al.* Composition of lung lavage in pulmonary alveolar microlithiasis. *Respiration* 1996; 63: 254–260.
68 Bignon J, Sebastien P, Gaudichet A, *et al.* Biological effects of attapulgite. *IARC Sci Publ* 1980; 30: 163–181.
69 Gellert AR, Kitajewska JY, Uthayakumar S, *et al.* Asbestos fibres in bronchoalveolar lavage fluid from asbestos workers: examination by electron microscopy. *Br J Ind Med* 1986; 43: 170–176.
70 Perna F, Iavarone M, Skrimpas S, *et al.* Detection and qualitative identification of mineral fibers and particles in alveolar macrophages of BAL fluid by SEM and EDXA. *Monaldi Arch Chest Dis* 2002; 57: 193–195.

71 Coetzee T. Pulmonary alveolar microlithiasis with involvement of the sympathetic nervous system and gonads. *Thorax* 1970; 25: 637–642.
72 Sandhyamani S, Verma K, Sharma SK, *et al.* Pulmonary alveolar microlithiasis. *Indian J Chest Dis Allied Sci* 1982; 24: 33–35.
73 Arslan A, Yalin T, Akan H, *et al.* Pulmonary alveolar microlithiasis associated with calcifications in the seminal vesicles. *J Belge Radiol* 1996; 79: 118–119.
74 Castellana G, Carone D, Castellana M. Microlithiasis of seminal vesicles and severe oligoasthenospermia in pulmonary alveolar microlithiasis (PAM): report of an unusual sporadic case. *Int J Fertil Steril* 2015; 9: 137–140.
75 Kanat F, Teke T, Imecik O. Pulmonary alveolar microlithiasis with epididymal and periurethral calcifications causing obstructive azospermia. *Int J Tuberc Lung Dis* 2004; 8: 1275.
76 Qublan H, Athamneh I, Al-Kaisi N. Azoospermia associated with testicular and pulmonary microlithiasis. *J Diagn Med Sonogr* 2003; 19: 192–194.
77 Qian X, Wu X, Liu X. Pulmonary alveolar microlithiasis with finger clubbing: a case report and literature review. *Exp Ther Med* 2016; 11: 1381–1384.
78 Griff S, Ammenwerth W, Schonfeld N, *et al.* Morphometrical analysis of transbronchial cryobiopsies. *Diagn Pathol* 2011; 6: 53.
79 Babiak A, Hetzel J, Krishna G, *et al.* Transbronchial cryobiopsy: a new tool for lung biopsies. *Respiration* 2009; 78: 203–208.
80 Thind GS, Bhatia JL. Pulmonary alveolar microlithiasis. *Br J Dis Chest* 1978; 72: 151–154.
81 Weinstein DS. Pulmonary sarcoidosis: calcified micronodular pattern simulating pulmonary alveolar microlithiasis. *J Thorac Imaging* 1999; 14: 218–220.
82 Sun HM, Chen F, Yin HL, *et al.* Rapid development of metastatic pulmonary calcifications in primary hyperparathyroidism: a case report and literature review. *Diagn Pathol* 2017; 12: 38.
83 Belem LC, Zanetti G, Souza AS, Jr., *et al.* Metastatic pulmonary calcification: state-of-the-art review focused on imaging findings. *Respir Med* 2014; 108: 668–676.
84 Ferreira F, Pereira e Silva JL, Hochhegger B, *et al.* Pulmonary alveolar microlithiasis. State-of-the-art review. *Respir Med* 2013; 107: 1–9.
85 Bhatia J, Thind G. Pulmonary alveolar microlithiasis. *Indian J Tuberculosis* 1976; 23: 110.
86 Ucan ES, Keyf AI, Aydilek R, *et al.* Pulmonary alveolar microlithiasis: review of Turkish reports. *Thorax* 1993; 48: 171–173.
87 Raffa H, El-Dakhakhny M, Al-Ibrahim K, *et al.* Single lung transplantation for alveolar micro-lithiasis: the first clinical report. *Saudi J Kidney Dis Transpl* 1996; 7: 189–193.
88 Reszka AA, Rodan GA. Mechanism of action of bisphosphonates. *Curr Osteoporos Rep* 2003; 1: 45–52.
89 Gocmen A, Toppare MF, Kiper N, *et al.* Treatment of pulmonary alveolar microlithiasis with a diphosphonate--preliminary results of a case. *Respiration* 1992; 59: 250–252.
90 Ozcelik U, Yalcin E, Ariyurek M, *et al.* Long-term results of disodium etidronate treatment in pulmonary alveolar microlithiasis. *Pediatr Pulmonol* 2010; 45: 514–517.
91 Ozcelik U, Gulsun M, Gocmen A, *et al.* Treatment and follow-up of pulmonary alveolar microlithiasis with disodium editronate: radiological demonstration. *Pediatr Radiol* 2002; 32: 380–383.
92 Cakir E, Gedik AH, Ozdemir A, *et al.* Response to disodium etidronate treatment in three siblings with pulmonary alveolar microlithiasis. *Respiration* 2015; 89: 583–586.
93 Allgrove J. Bisphosphonates. *Arch Dis Child* 1997; 76: 73–75.
94 Jankovic S, Pavlov N, Ivkosic A, *et al.* Pulmonary alveolar microlithiasis in childhood: clinical and radiological follow-up. *Pediatr Pulmonol* 2002; 34: 384–387.
95 Mariotta S, Guidi L, Papale M, *et al.* Pulmonary alveolar microlithiasis: review of Italian reports. *Eur J Epidemiol* 1997; 13: 587–590.
96 Chopra M, Tendolkar MS, Vardhan V. Case series of pulmonary alveolar microlithiasis from India. *BMJ Case Rep* 2019; 12: e227406.
97 Ganesan N, Ambroise MM, Ramdas A, *et al.* Pulmonary alveolar microlithiasis: an interesting case report with systematic review of Indian literature. *Front Med* 2015; 9: 229–238.
98 Ratjen FA, Schoenfeld B, Wiesemann HG. Pulmonary alveolar microlithiasis and lymphocytic interstitial pneumonitis in a ten-year-old girl. *Eur Respir J* 1992; 5: 1283–1285.
99 Yilmaz MI, Koc B, Kantarcioglu M, *et al.* Pulmonary alveolar microlithiasis after *Varicella zoster* infection in a patient presenting with antiphospholipid syndrome and discoid lupus. *Rheumatol Int* 2002; 22: 213–215.
100 Badger TL, Gottlieb L, Gaensler EA. Pulmonary alveolar microlithiasis, or calcinosis of the lungs. *N Engl J Med* 1955; 253: 709–715.
101 Peng T, Zhuo L, Wang Y, *et al.* Systematic review of sodium thiosulfate in treating calciphylaxis in chronic kidney disease patients. *Nephrology (Carlton)* 2018; 23: 669–675.
102 Strazzula L, Nigwekar SU, Steele D, *et al.* Intralesional sodium thiosulfate for the treatment of calciphylaxis. *JAMA Dermatol* 2013; 149: 946–949.
103 Hoeper MM, Andreas S, Bastian A, *et al.* Pulmonary hypertension due to chronic lung disease. Recommendations of the Cologne Consensus Conference 2010. *Pneumologie* 2011; 65: 208–218.
104 Freiberg DB, Young IH, Laks L, *et al.* Improvement in gas exchange with nasal continuous positive airway pressure in pulmonary alveolar microlithiasis. *Am Rev Respir Dis* 1992; 145: 1215–1216.
105 Palombini BC, da Silva Porto N, Wallau CU, *et al.* Bronchopulmonary lavage in alveolar microlithiasis. *Chest* 1981; 80: 242–243.
106 Shadmehr MB, Arab M, Pejhan S, *et al.* Eight years of lung transplantation: experience of the National Research Institute of Tuberculosis and Lung Diseases. *Transplant Proc* 2009; 41: 2887–2889.
107 Jackson KB, Modry DL, Halenar J, *et al.* Single lung transplantation for pulmonary alveolar microlithiasis. *J Heart Lung Transplant* 2001; 20: 226.
108 Borrelli R, Fossi A, Volterrani L, *et al.* Right single-lung transplantation for pulmonary alveolar microlithiasis. *Eur J Cardiothorac Surg* 2014; 45: e40.
109 Bonnette P, Bisson A, el Kadi NB, *et al.* Bilateral single lung transplantation. Complications and results in 14 patients. *Eur J Cardiothorac Surg* 1992; 6: 550–554.

110 Coulibaly B, Fernandez C, Reynaud-Gaubert M, *et al.* Alveolar microlithiasis with severe interstitial fibrosis leading to lung transplantation. *Ann Pathol* 2009; 29: 241–244.
111 Gucyetmez B, Ogan A, Cimet Ayyildiz A, *et al.* Lung transplantation in an intensive care patient with pulmonary alveolar microlithiasis - a case report. *F1000Res* 2014; 3: 118.
112 Jindal A, Rahulan V, Balasubramani G, *et al.* Pulmonary alveolar microlithiasis: a rare disease treated with lung transplantation, first case from India. *Lung India* 2019; 36: 546–549.
113 Shigemura N, Bermudez C, Hattler BG, *et al.* Lung transplantation for pulmonary alveolar microlithiasis. *J Thorac Cardiovasc Surg* 2010; 139: e50–e52.
114 Tachibana T, Hagiwara K, Johkoh T. Pulmonary alveolar microlithiasis: review and management. *Curr Opin Pulm Med* 2009; 15: 486–490.